BMC Neuroscience

RESEARCH ARTICLE

Open Access

Downregulation of calcium-dependent NMDA receptor desensitization by sodium-calcium exchangers: a role of membrane cholesterol

Dmitry A. Sibarov, Ekaterina E. Poguzhelskaya and Sergei M. Antonov*

Abstract

Background: The plasma membrane Na^+/Ca^{2+}-exchanger (NCX) has recently been shown to regulate Ca^{2+}-dependent *N*-methyl-D-aspartate receptor (NMDAR) desensitization, suggesting a tight interaction of NCXs and NMDARs in lipid nanoclasters or "rafts". To evaluate possible role of this interaction we studied effects of Li^+ on NMDA-elicited whole-cell currents and Ca^{2+} responses of rat cortical neurons in vitro before and after cholesterol extraction by methyl-β-cyclodextrin (MβCD).

Results: Substitution Li^+ for Na^+ in the external solution caused a concentration-dependent decrease of steady-state NMDAR currents from 440 ± 71 pA to 111 ± 29 pA in 140 mM Na^+ and 140 mM Li^+, respectively. The Li^+ inhibition of NMDAR currents disappeared in the absence of Ca^{2+} in the external solution (Ca^{2+}-free), suggesting that Li^+ enhanced Ca^{2+}-dependent NMDAR desensitization. Whereas the cholesterol extraction with MβCD induced a decrease of NMDAR currents to 136 ± 32 pA in 140 mM Na^+ and 46 ± 15 pA in 140 mM Li^+, the IC_{50} values for the Li^+ inhibition were similar (about 44 mM Li^+) before and after this procedure. In the Ca^{2+}-free Na^+ solution the steady-state NMDAR currents after the cholesterol extraction were 47 ± 6% of control values. Apparently this amplitude decrease was not Ca^{2+}-dependent. In the Na^+ solution containing 1 mM Ca^{2+} the Ca^{2+}-dependent NMDAR desensitization was greater when cholesterol was extracted. Obviously, this procedure promoted its development. In agreement, Li^+ and KB-R7943, an inhibitor of NCX, both considerably reduced NMDA-activated Ca^{2+} responses. The cholesterol extraction itself caused a decrease of NMDA-activated Ca^{2+} responses and, in addition, abolished the effects of Li^+ and KB-R7943. The cholesterol loading into the plasma membrane caused a recovery of the KB-R7943 effects.

Conclusions: Taken together our data suggest that NCXs downregulate the Ca^{2+}-dependent NMDAR desensitization. Most likely, this is determined by a tight functional interaction of NCX and NMDAR molecules because of their co-localization in membrane lipid rafts. The destruction of these rafts is accompanied by an enhancement of NMDAR desensitization and a loss of NCX-selective agent effects on NMDARs.

Keywords: NMDA receptors, Sodium-calcium exchanger, Lipid rafts, Desensitization, Glutamate

*Correspondence: antonov452002@yahoo.com
Sechenov Institute of Evolutionary Physiology and Biochemistry, Russian Academy of Sciences, pr. Torez 44 Saint-Petersburg, Russia

Background

N-methyl-D-aspartate activated glutamate receptors (NMDARs) are ligand gated ion channels which naturally transfer currents determined by Na^+, K^+ and Ca^{2+} permeation. High permeability of NMDARs to Ca^{2+} makes them involved in synaptic plasticity [1, 2], while their hyperactivation during ischemia or stroke causes neuronal Ca^{2+} overload and apoptosis [3]. Ca^{2+}-dependent desensitization of NMDARs represents a feedback regulation of the NMDAR open probability by the Ca^{2+} entry into neurons [4–8]. The Ca^{2+} entry via NMDAR pores produces a local increase of Ca^{2+} concentration (up to micromolar range) in a close proximity of receptor intracellular domains. Calmodulin binds free Ca^{2+} and then interacts with C-terminal domains of NMDAR GluN1 subunits causing the decrease of the channel open probability in the Ca^{2+} concentration-dependent manner because of Ca^{2+}-dependent NMDAR desensitization [9, for review see 10].

Recently it has been demonstrated that the inhibition of the plasma membrane Na^+/Ca^{2+} exchanger (NCX) either by KB-R7943 (2-[2-[4-(4-nitrobenzyloxy) phenyl] ethyl] isothiourea methanesulfonate) or by the substitution of Li^+ for Na^+ in the external physiological solution considerably enhances the Ca^{2+}-dependent desensitization of NMDARs [11]. As Li^+ is a substrate inhibitor of Na^+-dependent neurotransmitter transporters [12, 13] and exchangers [for review see 14] the substitution of Li^+ for Na^+ in the external solution decreases the efficacy of Ca^{2+} extrusion via NCX. The direct effects of Li^+ on NMDAR kinetics and conductance is negligible, because NMDARs have similar Li^+ and Na^+ channel permeabilities [15]. These observations suggest that NCX is involved in regulation of Ca^{2+}-dependent desensitization of NMDARs that could be achieved in the case of close location and interaction of NCX and NMDAR molecules in the plasma membrane.

The Li^+ therapy is widely used to stabilize mood disorders, including bipolar disorders and depression as well as suicidal behaviors [13]. There are some experimental indications that KB-R7943 reduces 4-aminopyridine-induced epileptiform activity in adult rats [16]. It is still not clear whether NCXs could represent a target of pharmacological action to compensate NMDAR-related neuronal pathologies and whether an acceleration of Ca^{2+}-dependent NMDAR desensitization by Li^+ is at least partially contributed to the Li^+ therapeutic effects. To provide more clues for understanding of these aspects of the NMDAR pharmacology here we study the concentration dependence of Li^+ effects on NMDAR currents and the role of functional interaction between NCXs and NMDARs that presumably requires their close spatial localization in lipid rafts.

Results

Lithium inhibition of NMDA-elicited currents

Cortical neurons in cultures express a variety of NCXs including NCX1-3 and NCKX isoforms [14]. Extracellular Li^+ represents a tool to cause the substrate inhibition of Na^+-dependent Ca^{2+} extrusion by all sodium-calcium exchanger subtypes. The stepwise proportional substitution of Li^+ for Na^+ in the bathing solution was used to obtain the dose-inhibition curve of NMDA-evoked currents for Li^+. With this particular aim the NMDA-activated currents were measured at 0, 21, 42, 70, 112 and 140 mM Li^+ in the bathing solution in the same experiment, where 140 mM Li^+ corresponded to 100% substitution of Li^+ for Na^+. An application of Li^+-containing solutions without agonists always preceded the application of the corresponding solution with NMDA. An increase of Li^+ concentrations in the external solution caused a decrease of NMDA-activated currents at the steady state (Fig. 1a). The control NMDA-evoked currents, measured at the steady state in the bathing solutions (140 mM Na^+) had the amplitude of 440.4 ± 71.9 pA ($n = 10$), that was significantly ($p < 0.001$, Student's two-tailed t test) larger compared to the corresponding value of 111.4 ± 29.1 pA ($n = 10$) measured at 140 mM Li^+ in the external solution. Dose-inhibition curves obtained from experiments were well fitted by Hill equation with IC_{50} of 46 ± 21 mM (Fig. 1b). Previously, we demonstrated that the inhibition of NMDA-activated currents by Li^+ is Ca^{2+}-dependent, because it could not be observed in the nominal absence of Ca^{2+} in the external solution [11]. Since Li^+ does not directly affect the NMDAR conductance and activation kinetics, as a substrate inhibitor of NCXs it could sufficiently decrease the efficacy of Ca^{2+} extrusion from neurons due to breaking ion transport by NCXs. The decrease of NMDAR current by Li^+ suggests that NCX contributes to the regulation of free Ca^{2+} concentration close to the inner membrane surface and the Ca^{2+}-dependent desensitization of NMDARs. This requires some functional interaction between NCXs and NMDARs that could occur if these molecules are located closely and interact within lipid nanoclasters or rafts.

The extraction of cholesterol from the plasma membrane by MβCD [17] is a widely used conventional procedure to destroy lipid nanoclusters. The treatment of neurons with 1.5 mM MβCD for 5 min was undertaken to extract cholesterol from membrane lipid rafts to achieve spatial uncoupling of NMDARs and NCXs. This procedure did not significantly alter the current–voltage relationships (I/V), suggesting the lack of its effect on the input resistance of neurons ($n = 5$, Fig. 1a). After the cholesterol extraction the mean amplitude of NMDA-evoked currents at the steady state in the Na^+-containing bathing

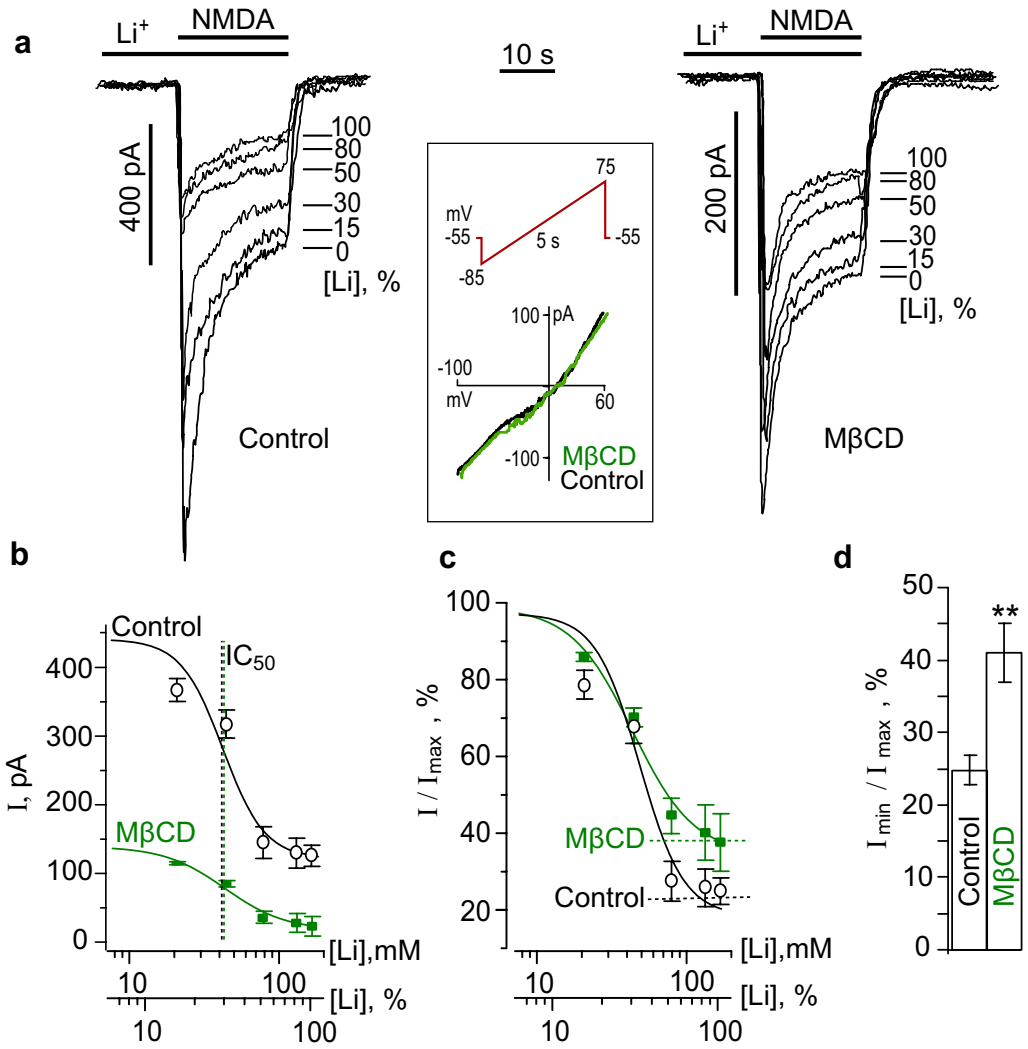

Fig. 1 Measurements of EC_{50} of Li^+ inhibition of NMDA-elicited currents before and after the cholesterol extraction. **a** Currents activated by 100 μM NMDA + 10 μM Gly recorded in the bathing solutions containing different Li^+ concentrations ([Li^+], % is indicated on the right of each trace) at − 55 mV before and after 5 min treatment with 1.5 mM MβCD. The insert in the box represents an example of I/V measurements before (black curve) and after (green curve) the MβCD treatment. The protocol of "ramp" is indicated by the red line above the records. **b** Concentration-inhibition curves for Li^+ of currents activated by 100 μM NMDA + 10 μM Gly. The mean values ± S.E.M. from 10 experiments for each of the conditions are plotted. Solid lines indicate fits of the data with the Hill equation with the parameters: $IC_{50} = 46 \pm 21$ mM and $h = 2.3 \pm 0.8$ ($n = 10$) in control conditions and 42 ± 20 mM and $h = 3.3 \pm 1.0$ ($n = 10$) after the MβCD treatment. Abscissa is the Li^+ concentration in the external solution presented as the absolute value ([Li^+], mM) and the ratio of [Li^+] to the sum of Na^+ and Li^+ concentrations of 140 mM ([Li^+], %). **c** The same curves as on (**b**) normalized to I_{max} to illustrate the difference in the extent of the Li^+ inhibition of currents, activated by NMDA before and after the MβCD treatment. **d** Histogram of fractions of residual currents (I_{min}) obtained at 140 mM Li^+ ([Li^+], 100%) in the external solution before (control) and after the MβCD treatment (MβCD) to the value of I_{max}, drown from the fits (mean values ± S.E.M. for each of the conditions, $n = 10$). ** the value is significantly different from the corresponding value obtained under control conditions ($p < 0.01$, Student's two-tailed *t*-test)

solution was 136.8 ± 32.8 pA ($n = 10$), revealing its decrease in comparison to MβCD untreated neurons as control conditions ($p < 0.007$, Student's two-tailed *t* test, Fig. 1a, b). The stepwise substitution of Li^+ for Na^+ in the external solution after the MβCD treatment further decreased the NMDA-evoked currents to the mean steady-state amplitude of 46.8 ± 15.3 pA ($n = 10$, $p < 0.008$, Student's two-tailed *t*-test). The IC_{50} value for the Li^+ inhibition of NMDA-activated currents after the MβCD treatment was 42 ± 20 mM (Fig. 1b, c) which did not differ significantly from the value obtained under the control conditions (on MβCD untreated neurons). It should be noted, however, that the degree of the NMDAR current inhibition in the Li^+-containing bathing solution was less pronounced after

the MβCD treatment than before this procedure and were 59 ± 4% ($n = 10$) and 77 ± 3% ($n = 10$) inhibition ($p < 0.03$, Student's two-tailed *t*-test), respectively (Fig. 1d). Presumably, spatial uncoupling of NCXs and NMDARs limits the effect of the NCX inhibition on NMDAR currents. This could be the case, if NCXs maintain low intracellular free Ca^{2+} concentration in the close proximity of NMDARs, which prevents the development of Ca^{2+}-dependent inactivation of NMDARs.

Calcium-dependent and -independent effects of cholesterol extraction on NMDARs

The interpretation of the above data that the cholesterol extraction may accelerate the Ca^{2+}-dependent desensitization destroying membrane lipid rafts and NCX-NMDAR interplay becomes less evident in a view of the recent observation that cholesterol is important for the NMDAR functioning and its extraction provokes the ligand-dependent desensitization of NMDARs [17]. In order to distinguish between Ca^{2+}-dependent and -independent mechanisms the effects of cholesterol extraction by MβCD on NMDA-activated currents were evaluated in the presence of 1 mM Ca^{2+} and in the nominal absence of Ca^{2+} in the bathing solution (Fig. 2a).

In the absence of Ca^{2+} in the external solution the ratio of amplitudes of NMDA-activated steady-state currents, recorded after and before 5 min MβCD treatment was 47 ± 6% ($n = 6$). The decrease of the steady-state amplitudes of NMDAR currents after the treatment is caused by the direct effect of the cholesterol extraction on NMDARs, because under these particular conditions the Ca^{2+}-dependent desensitization was not observed (Fig. 2a). In the presence of 1 mM Ca^{2+} in the bathing solution, however, the Ca^{2+}-dependent desensitization of NMDARs, measured as the ratio of the steady-state amplitudes of currents in the presence and absence of Ca^{2+} before and after the MβCD treatment was significantly greater when cholesterol was extracted (Fig. 2a, b), suggesting that this procedure enhanced the Ca^{2+}-dependent NMDAR desensitization. In addition, we performed similar experiments on neurons patched with 1 mM BAPTA in the pipette solution. Under these particular conditions the Ca^{2+}-dependent desensitization of NMDARs was not observed both in the presence and absence of Ca^{2+} in the external bathing solution (Fig. 2c). The direct effect of MβCD treatment on NMDARs was pronounced and the ratio values obtained in the presence and absence of external Ca^{2+} were similar (Fig. 2c, d). In 1 mM intrapipette BAPTA the steady-state NMDAR currents decreased after the extraction to about 10% of their amplitudes (Fig. 2d), whereas in experiments when the intracellular media was natural in terms of Ca^{2+} buffering the NMDAR currents decreased in a much lesser extent (about 47%, Fig. 2a).

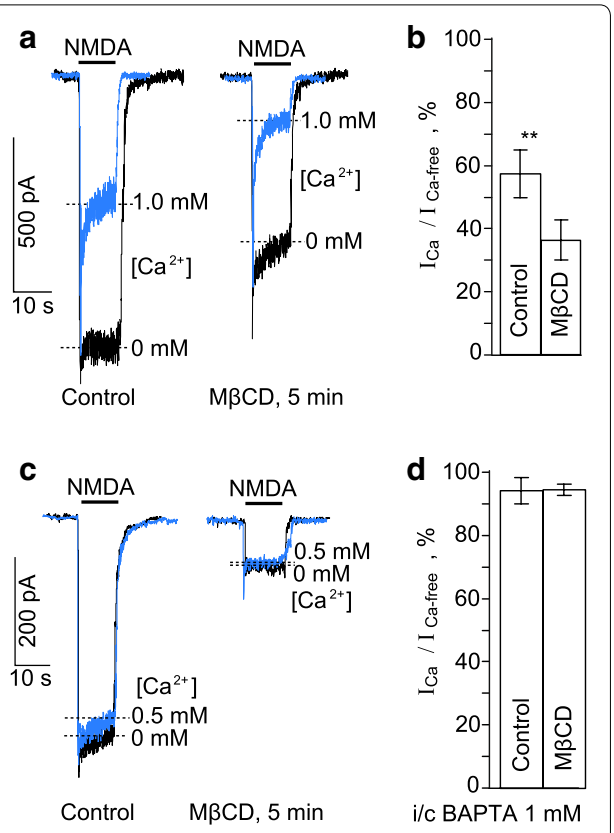

Fig. 2 Effects of the cholesterol extraction on NMDAR currents. **a** Currents activated by 100 μM NMDA + 10 μM Gly recorded in the same neuron at − 55 mV in the nominal absence of Ca^{2+} and presence of 1 mM Ca^{2+} in the bathing solution before (Control) and after the cholesterol extraction with 1.5 mM MβCD (MβCD, 5 min). Overlays of currents are presented for the better comparison of their kinetics. **b** Comparison of NMDAR Ca^{2+}-dependent desensitization before (Control) and after the cholesterol extraction (MβCD). On the histogram the amplitude ratio of currents recorded in the presence of 1 mM Ca^{2+} (I_{Ca}) and the absence of Ca^{2+} ($I_{Ca\text{-}free}$) in the external solution measured at the steady state (mean values ± S.E.M. for each of the conditions, $n = 6$). ** the value is significantly different for the corresponding value obtained after the cholesterol extraction (MβCD, $p < 0.007$, Student's two-tailed *t*-test). **c** Currents activated by 100 μM NMDA + 10 μM Gly recorded in the same neuron at − 55 mV in the nominal absence of Ca^{2+} and presence of 0.5 mM Ca^{2+} in the bathing solution using the 1 mM BAPTA- containing intrapipette solution before (Control) and after the cholesterol extraction with 1.5 mM MβCD (MβCD, 5 min). Overlays of currents are presented for the better comparison of their kinetics. **d** Comparison of the NMDAR Ca^{2+}-dependent desensitization of currents recorded using the 1 mM BAPTA-containing intrapipette solution before (Control) and after the cholesterol extraction (MβCD). On the histogram the amplitude ratio of currents recorded in the presence of 0.5 mM Ca^{2+} (I_{Ca}) and the absence of Ca^{2+} ($I_{Ca\text{-}free}$) in the external solution measured at the steady state (mean values ± S.E.M. for each of the conditions, $n = 6$)

Based on these experiments we may assume that in lipid rafts NCX weakens Ca^{2+}-dependent desensitization of NMDARs by quick extrusion of local intracellular Ca^{2+} entering neurons via open NMDAR pores. It is likely, that the destruction of lipid rafts increases the distance between NCXs and NMDARs allowing intracellular Ca^{2+} accumulation close to the NMDAR intracellular domains which enhances their Ca^{2+}-dependent desensitization. Pronounced Ca^{2+}-dependent desensitization of NMDARs, however, should provide a feed back regulation to limit the cytoplasmic Ca^{2+} accumulation during the NMDA action on neurons.

NCX inhibition and NMDA-elicited cytoplasmic Ca^{2+} accumulation

To provide additional experimental support in favor of mechanisms suggested, the effects of NCX inhibition with 140 mM Li^+ or KB-R7943 before and after the cholesterol extraction by MβCD (1.5 mM for 5 min) on intracellular Ca^{2+} responses to 2 min NMDA applications were studied. For quantitative comparison of effects we evaluated an integral of Ca^{2+}-induced fluorescence, which has to be proportional to the Ca^{2+} entry through open NMDAR channels and, therefore, to the amplitudes of NMDA-activated currents. As in electrophysiological experiments, the Li^+-containing bathing solution was applied alone and than with NMDA to equilibrate neurons and check pure Li^+ effects for possible further data correction (Fig. 3a). When NMDA was applied in the Li^+-containing bathing solution Ca^{2+} responses of neurons decreased to 54 ± 2% (overall 98 neurons, $n = 3$) of Ca^{2+} responses recorded in the Na^+-containing bathing solution ($p < 0.001$, Student's t test). This observation is consistent with the Li^+ effect on NMDA-activated currents. After the MβCD treatment the Ca^{2+} responses to NMDA in the Na^+-containing solution were 35 ± 9% (overall 98 neurons, $n = 3$) and in the Li^+-containing solution were 36 ± 9% (overall 98 neurons, $n = 3$) of the Ca^{2+} responses, obtained before the treatment in the Na^+-containing solution (Fig. 3a and b). Because these values were significantly smaller, than those obtained before the treatment in the Na^+ solution ($p < 0.0001$, one-way paired ANOVA) and did not differ between each other (Bonferroni post hoc test) we conclude that the MβCD treatment abolished the effects of Li^+ on NMDARs.

Thus, spatial uncoupling of NMDARs and NCXs resulted in the decrease of Ca^{2+} entry via NMDARs. Inhibition of NCX with Li^+ after the cholesterol extraction was not able to decrease NMDAR mediated Ca^{2+} accumulation.

We further performed the Ca^{2+} imaging experiments in which KB-R7943 (10 μM) as a specific NCX inhibitor, was utilized instead of the Li^+ solution. In the Na^+-containing external solution combined applications of NMDA with KB-R7943 induced Ca^{2+} responses that corresponded to 59 ± 5% (overall 91 neurons, $n = 3$) of NMDA-elicited Ca^{2+} responses and differed from them significantly ($p < 0.001$, one-way paired ANOVA) (Fig. 3c). This observation is consistent with the KB-R7943 effect on NMDA-activated currents [11]. The MβCD treatment decreased the NMDA-elicited Ca^{2+} responses both in the absence and presence of KB-R7943 to 32 ± 8% and 24 ± 7% (overall 91 neurons, $n = 3$), respectively (Fig. 3d). These values are not significantly different (Bonferroni post hoc test) suggesting that the cholesterol extraction abolished the KB-R7943 effects on NMDA-activated currents. To validate that the effects of MβCD treatment are actually caused by the cholesterol loss from the plasma membrane, cholesterol-MβCD, as a cholesterol donor, was applied for 30 min after the effects of MβCD were achieved (Fig. 3c). Loading of cholesterol into the plasma membrane both increased the amplitudes of Ca^{2+}-responses to NMDA and recovered the inhibitory effect of KBR (Fig. 3c, d).

Therefore, the effects of Li^+ and KB-R7943 on NMDA-elicited Ca^{2+} responses of neurons coincide well suggesting that they both are realizing through the influence of NCX on the Ca^{2+}-dependent desensitization of NMDARs.

Discussion

In spite of a large number of novel pharmacological agents has recently appeared, Li^+ has still broad usage as a tool of neuroscience researches, since it can affect key functional processes of the central nervous system (CNS) including different enzymes [for review see 13] and Na^+-dependent neurotransmitter transporters [12] and exchangers [for review see 14]. Diverse and complex action of Li^+ on the human CNS is highlighted by the Li^+ therapy which is widely utilized to stabilize many mental disorders. Usually therapeutic Li^+ concentrations in the blood vary within the range of 0.6–1.2 mM and the concentrations over 1.5 mM are thought to become toxic [for review see 13]. In addition it has been demonstrated recently that the substitution of Li^+ for Na^+ in the external solution in the presence of Ca^{2+} causes considerable decrease of currents activated by NMDA [11]. This somehow contradicts to the lack of the NMDAR Li^+ inhibition in the absence of Ca^{2+} in the external solution [11] and to the observation that Li^+ does not influence the NMDAR conductance and activation kinetics [15]. The IC_{50} value for the Li^+ inhibition of NMDA-activated currents measured here is about 44 mM. It is, therefore, unlikely that the Li^+ inhibition of NMDAR currents in some extent

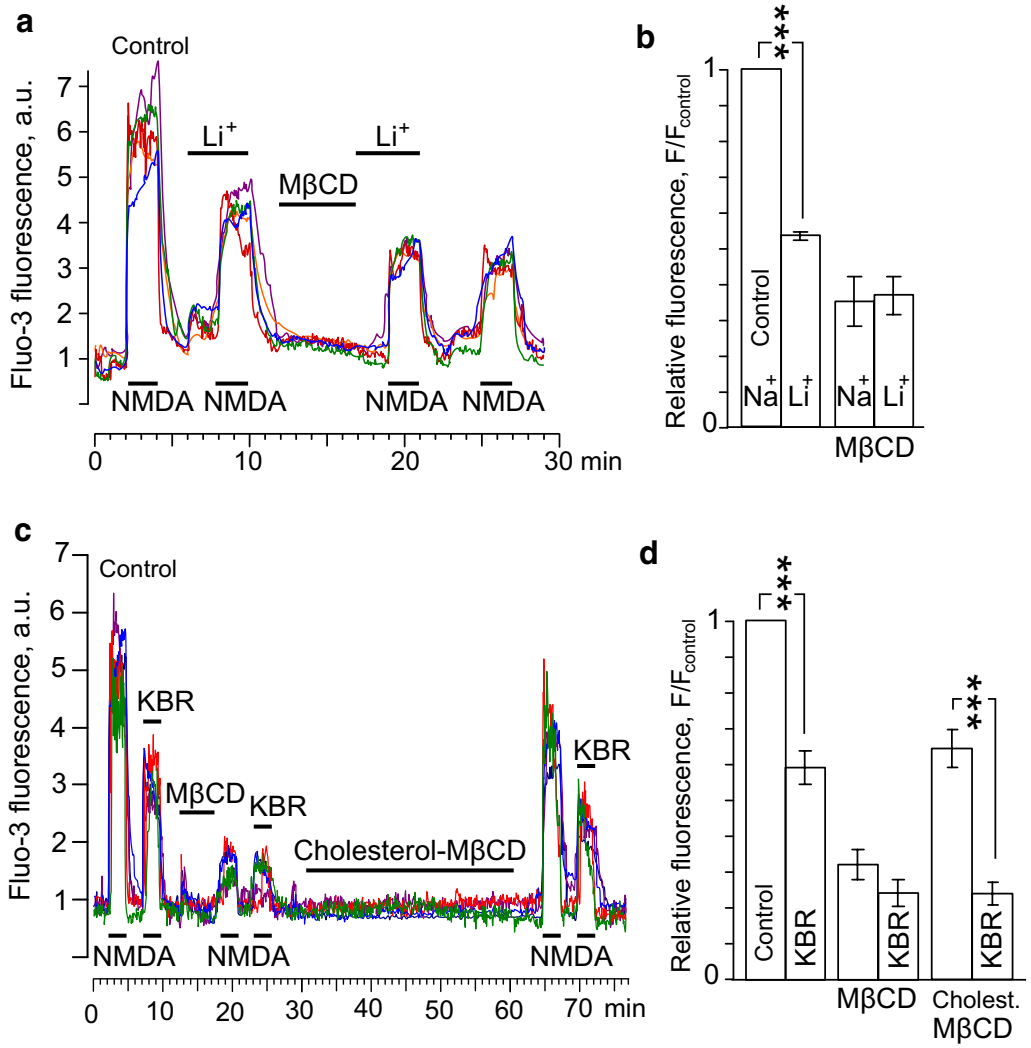

Fig. 3 Effects of the cholesterol extraction and loading on Ca^{2+} responses induced by NMDA. **a** Neuronal Ca^{2+} responses evoked by 100 μM NMDA + 10 μM Gly in the 140 mM Na^+-containing (Control) and 140 mM Li^+-containing external solutions before and after the cholesterol extraction. Applications of 100 μM NMDA + 10 μM Gly, 140 mM Li^+ and 1.5 mM MβCD are indicated by bars. Examples of Ca^{2+} responses of 4 neurons are shown. **b** The histogram represents the ratio of squares of Ca^{2+} responses to the square of Ca^{2+} response obtained under control (140 mM Na^+-containing external solution). Mean values ± S.E.M. for each of the conditions (overall 98 neurons, $n = 3$) are plotted. *** the value is significantly different from other data ($p < 0.0001$, one-way paired ANOVA, Bonferroni post hoc test). **c** Neuronal Ca^{2+} responses recorded in 140 mM Na^+-containing external solution evoked by 100 μM NMDA + 10 μM Gly (Control) and 100 μM NMDA + 10 μM Gly + 10 μM KB-R7943 (KBR) before cholesterol extraction, after cholesterol depletion with MβCD and then after cholesterol restoration with cholesterol-MβCD. Applications of 100 μM NMDA + 10 μM Gly, 10 μM KB-R7943, 1.5 mM MβCD and 1.5 mM cholesterol-MβCD are indicated by bars. Examples of Ca^{2+} responses of 6 neurons are shown. **d** The histogram represents the ratio of squares of Ca^{2+} responses to the square of Ca^{2+} response obtained under control (NMDA). Mean values ± S.E.M. for each of the conditions (overall 91 neurons, $n = 3$) are plotted. *** the value is significantly different from other data ($p < 0.0001$, one-way paired ANOVA, Bonferroni post hoc test)

contributes in the therapeutic effect during the Li^+ therapy, whereas the mechanism of the Ca^{2+}-dependent Li^+ inhibition of NMDARs requires further consideration.

The critical dependence of Li^+ inhibition of NMDAR currents on extracellular Ca^{2+} forced us to the conclusion that Li^+ inhibits NMDARs indirectly breaking the Ca^{2+} extrusion from neurons by NCXs, which are involved in regulation of pre-membrane Ca^{2+} concentration in the close proximity to the NMDAR intracellular domains during Ca^{2+} entry through the channels of activated NMDARs. By the other words Li^+ promotes Ca^{2+}-dependent desensitization of NMDARs inhibiting the NCX transport of Ca^{2+} from neurons [11]. If this is the case then NMDARs and NCXs should co-localize

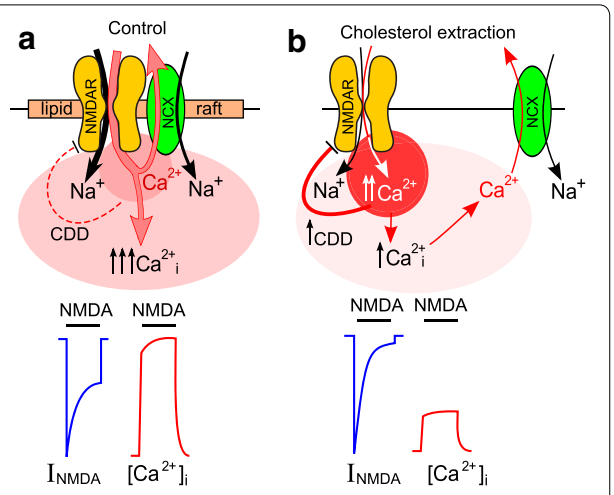

Fig. 4 Schematics of the data interpretation. **a** In control conditions local Ca^{2+} accumulation in the close proximity to intracellular domains of activated NMDARs is prevented by NCX-transported Ca^{2+} extrusion. The integral Ca^{2+} entry into neurons via activated NMDARs is large because of moderate Ca^{2+}-dependent NMDAR desensitization (CDD). This causes prominent cytozolic $[Ca^{2+}]_i$ increase ($\uparrow\uparrow\uparrow Ca^{2+}_i$). Typical whole-cell current (I_{NMDA}) and fluorescent Ca^{2+} probe response are indicated below the panel. **b** The destruction of lipid rafts increases a distance between NMDARs and NCXs which prevents fast removal of Ca^{2+} entering via open NMDAR channels. Local Ca^{2+} accumulation in the close proximity of intracellular domains of activated NMDAR enhances their CDD and limits NMDAR current steady-state amplitude and as a consequence weakens total cytosolic Ca^{2+} accumulation. Typical whole-cell current (I_{NMDA}) and fluorescent Ca^{2+} probe response ($[Ca^{2+}]_i$) are indicated below the panel. For further explanation, see "Discussion" section

and interact that could be achieved in membrane cholesterol rich nanoclusters or lipid rafts (Fig. 4a). Actually the co-localization of NMDARs and NCXs in lipid rafts at the distance less than 80 nm was recently demonstrated using FRET (Förster Resonance Energy Transfer) experiments [18, 19]. In our experiments the cholesterol extraction, that is known to destruct lipid rafts, resulted in a substantial decrease of NMDAR currents, which is consistent to the earlier observation [17], but did not cause significantly changes of the IC_{50} value for the Li^+ inhibition of NMDAR currents. This may suggest that the cholesterol extraction does not influence the transport by NCXs [20] and similar Li^+ concentrations are required to inhibit NCXs before and after the MβCD treatment.

The requirement of cholesterol for functioning of NMDARs was recently demonstrated [17], because its extraction induced fast ligand-dependent NMDAR desensitization. In agreement when we used 1 mM BAPTA containing intrapipette solution (calculated free Ca^{2+} concentration is 13 nM) a tenfold decrease of NMDAR currents and a lack of Ca^{2+}-dependent NMDAR desensitization were observed. NMDA-activated currents recorded in the absence of Ca^{2+} in the external solution using the BAPTA-free intrapipette solution did not reveal the NMDAR Ca^{2+}-dependent desensitization as well. The cholesterol extraction under these conditions, however, induced a twofold decrease of the NMDAR currents. The lesser extent of the ligand-dependent desensitization obtained without BAPTA may suggest that some normal level of free Ca^{2+} in the cytoplasm is required for NMDAR functioning. In addition the extraction caused an enforcement of Ca^{2+}-dependent NMDAR desensitization suggesting that the disaggregation of molecules within destructed lipid rafts is accompanied by the disruption of NCX regulated Ca^{2+} pre-membrane balance.

Measurements of intracellular Ca^{2+} dynamics revealed that the NCX inhibition with Li^+ or KB-R7943 significantly decreased the NMDA-elicited Ca^{2+} responses, which is consistent to their effects on currents, activated by NMDA. In agreement to previous observations [21] the cholesterol extraction caused the decrease of the cytoplasm Ca^{2+} accumulation, and furthermore abolished the effects of both Li^+ and KB-R7943 on the neuronal Ca^{2+} cytoplasmic responses. The cholesterol loading into the plasma membrane was followed by the recovery of Ca^{2+}-response amplitudes and, most importantly, restored the NCX effects on the Ca^{2+}-dependent NMDAR desensitization. These further support our conclusion that the destruction of lipid rafts abolishes the influence of NCXs on NMDARs (Fig. 4b), which is consistent to modeling of interaction between CaM and C-terminal of NMDAR GluN1 subunits that requires molecule co-localization within the distance of tens of nanometers [22].

Thus, our observations considerably widen the range of pharmacological agents which may indirectly influence NMDAR functioning through the metabolism of cholesterol or the inhibition of NCX, that presumably could potentiate the Ca^{2+}-desensitization of NMDARs.

Conclusions

Thus, the NCX inhibition prevents the maintainance of low Ca^{2+} level in the proximity of the intracellular domains of NMDARs by the Ca^{2+} extrusion to the outside, which elevates pre-membrane local Ca^{2+} concentration, but limits total Ca^{2+} entry into neurons. Spatial uncoupling of NCXs and NMDARs by cholesterol extraction enhances the NMDAR Ca^{2+}-dependent desensitization abolishing its regulation by NCXs and is accompanied by a loss of NCX-selective agent effects on NMDARs. As a consequence the inhibition of NCXs with Li^+ or KB-R7943 after the cholesterol extraction

does not significantly influence the cytoplasmic Ca^{2+} accumulation in response to NMDAR activation.

Methods

Primary culture of cortical neurons

The culture preparation from rat embryos was previously described [23, 24]. All procedures using animals were in accordance with recommendations of the Federation for Laboratory Animal Science Associations and approved by the Bioethics Committee of Sechenov Institute of Evolutionary Physiology and Biochemistry of the Russian Academy of Sciences (IEPhB RAS). Wistar rats were maintained on a 12 h day/night cycle at constant room temperature with ad libitum access to water and standard rat fodder in the animal facility of the IEPhB RAS. Experiments were designed to minimize the number of animals used in research.

Overall 12 Wistar rats 16 days pregnant were used for experiments. The pregnant rat was placed into the plastic box connected by a tube with CO_2 tank and then sacrificed by 30–40 s CO_2 inhalation. Immediately after cardiac arrest fetuses were removed and their cerebral cortices were isolated, enzymatically dissociated and used to prepare primary neuronal cultures. Cells were used for experiments after 10–15 days in culture [24, 25]. Cells were grown in Neurobasal™ culture media supplemented with B-27 (Gibco-Invitrogen, UK) on glass coverslips coated with poly-D-lysine.

Patch clamp recordings

Whole-cell currents were recorded on rat cortical neurons in primary culture (10–15 days in vitro) by patch clamp technique using a MultiClamp 700B amplifier with Digidata 1440A acquisition system. Details of recording and fast perfusion system were described previously [26]. Unless otherwise specified, the following extracellular medium was used for recording (external bathing solution, in mM): 140 NaCl; 2.8 KCl; 1.0 $CaCl_2$; 10 HEPES, at pH 7.2–7.4. The patch-pipette solution contained (in mM): 120 CsF, 10 CsCl, 10 EGTA, and 10 HEPES. In some experiments BAPTA ((1,2-bis(*o*-aminophenoxy) ethane-*N*,*N*,*N*′,*N*′-tetraacetic acid) was added to path-pipette solution to prevent calcium-dependent desensitization of NMDARs. This solution contained (in mM): 120 CsF, 10 CsCl, 10 EGTA, 10 HEPES, 0.1 $CaCl_2$, 1 BAPTA to achieve calculated free $[Ca^{2+}]$ of 13 nM. The pH was adjusted to 7.4 with CsOH. Measured osmolarities of the external bathing solution and the patch-pipette solution were 310 and 300 mOsm, respectively. Patch pipettes (2–4 MΩ) were pulled from 1.5-mm (outer diameter) borosilicate standard wall capillaries with inner filament (Sutter Instrument, Novato, CA, USA). In whole-cell configuration the series resistances did not exceed 10 MΩ. Holding membrane voltage (V_m) was corrected for the liquid junction potential between the Na^+-containing external bathing solution and the Cs^+-containing pipette solution of − 15 mV.

Loading of Fluo-3 AM and Ca^{2+} imaging

Cells were loaded with Fluo-3 AM (4 mM, Life Technologies, Foster City, CA, USA) using conventional protocols as described previously [27]. Coverslips with Fluo-3-loaded neurons were placed in the perfusion chamber, which was mounted on the stage of a Leica TCS SP5 MP inverted microscope (Leica Microsystems, Germany). Fluorescence was activated with 488 nm laser light and emission was measured within the wavelength range from 500 to 560 nm. Images were captured every 1.5 s during 30 min experiments.

Drugs

Functional activity of NMDARs requires binding of both glutamate and a co-agonist, glycine. Unless otherwise stated, to activate NMDARs we applied 100 μM NMDA with 10 μM L-glycine (Gly). KB-R7943 (2-[4-[(4-nitrophenyl)methoxy]phenyl]ethyl ester, methanesulfonate, 10 μM) application or proportional substitution of Li^+ for Na^+ in the external bathing solution were used to inhibit NCX. Methyl-β-cyclodextrin (MβCD, 1.5 mM) application for 5 min was used to destruct lipid rafts by extracting cholesterol from the plasma membrane. The complex of cholesterol with methyl-β-cyclodextrin (cholesterol-MβCD, 1.5 mM) as a donor of cholesterol was applied for 30 min to restore the cholesterol content of the plasma membrane. All compounds were from Sigma-Aldrich, St. Louis, MO, USA or Tocris Bioscience, UK.

Data analysis

Quantitative data are expressed as mean ± SEM. ANOVA and Bonferroni multiple comparison methods as well as Student's two-tailed *t*-test were used for statistical analysis. Number of experiments is indicated by *n* throughout. In the patch-clamp experiments *n* represents a number of recorded neurons. In the Ca^{2+}-imaging experiments *n* represents a number of used culture coverslips. From every coverslip a single mean value obtained from many cells was utilized for statistics. The data were considered as significantly different based on a confidence level of 0.05. Current measurements were plotted using ClampFit 10.2 (Molecular Devices). The IC_{50} (half maximal inhibitory concentration) and Hill coefficient (h) for inhibition of NMDA-evoked currents with Li^+ were estimated by fitting of concentration–response curves with the Hill equation, $I = I_{min} + (I_{max} - I_{min})/(1 + [Li^+]^h/IC_{50}^h)$, where the I_{max} and I_{min} are the current of maximal and minimal amplitudes elicited by NMDA at different $[Li^+]$.

Abbreviations
KB-R7943: (2-[4-[(4-nitrophenyl)methoxy]phenyl]ethyl ester, methanesulfonate; MβCD: Methyl-β-cyclodextrin; NCX: Na^+/Ca^{2+}-exchanger; NMDAR: *N*-methyl-D-aspartate receptor.

Authors' contributions
EEP and DAS performed experiments. DAS supervised data acquisition and statistical analysis. DAS and SMA are responsible for the data interpretation and wrote the paper. SMA is responsible for critically revising the manuscript for intellectual content. All authors read and approved the final manuscript.

Acknowledgements
Imaging experiments were performed at Center for Collective Use of Sechenov Institute of Evolutionary Physiology and Biochemistry of the Russian Academy of Sciences.

Competing interests
The authors declare that they have no competing interests.

Availability of data and materials
The datasets used during the study are included in the published article. Source patch-clamp recordings and imaging data are available at the institutional database and can be made available from the corresponding author upon request.

Consent for publication
Not applicable.

Ethics approval and consent to participate
All the experiments with rats were approved by the Bioethics Committee of Sechenov Institute of Evolutionary Physiology and Biochemistry of the Russian Academy of Sciences (IEPhB RAS).

Funding
This work was supported by Russian Science Foundation Grant #16-15-10192.

Publisher's Note

Received: 5 September 2018 Accepted: 6 November 2018
Published online: 12 November 2018

References
1. Bliss TVP, Collingridge GL. A synaptic model of memory: long-term potentiation in the hippocampus. Nature. 1993;361:31–9. https://doi.org/10.1038/361031a0.
2. Bear MF. Mechanism for a sliding synaptic modification threshold. Neuron. 1995;15:1–4. https://doi.org/10.1016/0896-6273(95)90056-X.
3. Choi DW. Calcium: still center-stage in hypoxic-ischemic neuronal death. Trends Neurosci. 1995;18:58–60. https://doi.org/10.1016/0166-2236(95)80018-W.
4. Mayer ML, Westbrook GL. The action of *N*-methyl-D-aspartic acid on mouse spinal neurones in culture. J Physiol. 1985;361:65–90. https://doi.org/10.1113/jphysiol.1985.sp015633.
5. Zorumski CF, Yang J, Fischbach GD. Calcium dependent, slow desensitization distinguishes different types of glutamate receptors. Cell Mol Neurobiol. 1989;9:95–104. https://doi.org/10.1007/BF00711446.
6. Legendre P, Rosenmund C, Westbrook GL. Inactivation of NMDA channels on hippocampal neurons by intracellular calcium. J Neurosci. 1993;13:674–84. https://doi.org/10.1523/JNEUROSCI.13-02-00674.1993.
7. Vyklický LJ. Calcium-mediated modulation of *N*-methyl-D-aspartate (NMDA) responses in cultured rat hippocampal neurones. J Physiol. 1993;470:575–600. https://doi.org/10.1113/jphysiol.1993.sp019876.
8. Medina I, Filippova N, Charton G, Rougeole S, Ben-Ari Y, Khrestchatisky M, Bregestovski P. Calcium-dependent inactivation of heteromeric NMDA receptor-channels expressed in human embryonic kidney cells. J Physiol. 1995;482:567–73. https://doi.org/10.1113/jphysiol.1995.sp020540.
9. Ehlers MD, Zhang S, Bernhadt JP, Huganir RL. Inactivation of NMDA receptors by direct interaction of calmodulin with the NR1 subunit. Cell. 1996;84(5):745–55. https://doi.org/10.1016/S0092-8674(00)81052-1.
10. Sibarov DA, Antonov SM. Calcium dependent desensitization of NMDA receptors. Biochemistry (Moscow). 2018;83(10):1173–83.
11. Sibarov DA, Abushik PA, Poguzhelskaya EE, Bolshakov KV, Antonov SM. Inhibition of plasma membrane Na/Ca-exchanger by KB-R7943 or lithium reveals its role in Ca-dependent NMDAR inactivation. J Pharmacol Exp Ther. 2015;355(3):484–95. https://doi.org/10.1124/jpet.115.227173.
12. Antonov SM, Magazanik LG. Intense non-quantal release of glutamate in an insect neuromuscular junction. Neurosci Lett. 1988;93:204–8. https://doi.org/10.1016/0304-3940(88)90082-1.
13. Can A, Schulze TG, Gould TD. Molecular actions and clinical pharmacogenetics of lithium therapy. Pharmacol Biochem Behav. 2014;123:3–16. https://doi.org/10.1016/j.pbb.2014.02.004.
14. Török TL. Electrogenic Na^+/Ca^{2+}-exchange of nerve and muscle cells. Prog Neurobiol. 2007;82:287–347. https://doi.org/10.1016/j.pneurobio.2007.06.003.
15. Karkanias NB, Papke RL. Subtype-specific effects of lithium on glutamate receptor function. J Neurophysiol. 1999;81:1506–12. https://doi.org/10.1152/jn.1999.81.4.1506.
16. Hernandez-Ojeda M, Ureña-Guerrero ME, Gutierrez-Barajas PE, Cardenas-Castillo JA, Camins A, Beas-Zarate C. KB-R7943 reduces 4-aminopyridine-induced epileptiform activity in adult rats after neuronal damage induced by neonatal monosodium glutamate treatment. J Biomed Sci. 2017;24(1):27. https://doi.org/10.1186/s12929-017-0335-y.
17. Korinek M, Vyklicky V, Borovska J, Lichnerova K, Kaniakova M, Krausova B, et al. Cholesterol modulates open probability and desensitization of NMDA receptors. J Physiol. 2015;593(10):2279–93. https://doi.org/10.1113/jphysiol.2014.288209.
18. Marques-da-Silva D, Gutierrez-Merino C. L-type voltage-operated calcium channels, *N*-methyl-D-aspartate receptors and neuronal nitric-oxide synthase form a calcium/redox nano-transducer within lipid rafts. Biochem Biophys Res Commun. 2012;420:257–62. https://doi.org/10.1016/j.bbrc.2012.02.145.
19. Marques-da-Silva D, Gutierrez-Merino C. Caveolin-rich lipid rafts of the plasma membrane of mature cerebellar granule neurons are microcompartments for calcium/reactive oxygen and nitrogen species cross-talk signaling. Cell Calcium. 2014;56(2):108–23. https://doi.org/10.1016/j.ceca.2014.06.002.
20. Bossuyt J, Taylor BE, James-Kracke M, Hale CC. Evidence for cardiac sodium-calcium exchanger association with caveolin-3. FEBS Lett. 2002;511(1–3):113–7. https://doi.org/10.1016/S0014-5793(01)03323-3.
21. Frank C, Giammarioli AM, Pepponi R, Fiorentini C, Rufini S. Cholesterol perturbing agents inhibit NMDA-dependent calcium influx in rat hippocampal primary culture. FEBS Lett. 2004;566(1–3):25–9. https://doi.org/10.1016/j.febslet.2004.03.113.
22. Iacobucci GJ, Popescu GK. Resident calmodulin primes NMDA receptors for Ca-dependent inactivation. Biophys J. 2017;113(10):2236–48. https://doi.org/10.1016/j.bpj.2017.06.035.
23. Antonov SM, Gmiro VE, Johnson JW. Binding sites for permeant ions in the channel of NMDA receptors and their effects on channel block. Nat Neurosci. 1998;1:451–61. https://doi.org/10.1038/2167.
24. Mironova EV, Evstratova AA, Antonov SM. A fluorescence vital assay for the recognition and quantification of excitotoxic cell death by necrosis and apoptosis using confocal microscopy on neurons in culture. J Neurosci Methods. 2007;163:1–8. https://doi.org/10.1016/j.jneumeth.2007.02.010.
25. Han EB, Stevens CF. Development regulates a switch between post- and presynaptic strengthening in response to activity deprivation. Proc Natl Acad Sci USA. 2009;106:10817–22. https://doi.org/10.1073/pnas.0903603106.
26. Sibarov DA, Abushik PA, Giniatullin R, Antonov SM. GluN2A Subunit-containing NMDA receptors are the preferential neuronal targets of homocysteine. Front Cell Neurosci. 2016;10:246. https://doi.org/10.3389/fncel.2016.00246.
27. Abushik PA, Sibarov DA, Eaton MJ, Skatchkov SN, Antonov SM. Kainate-induced calcium overload of cortical neurons in vitro: dependence on expression of AMPAR GluA2-subunit and down-regulation by subnanomolar ouabain. Cell Calcium. 2013;54:95–104. https://doi.org/10.1016/j.ceca.2013.05.002.